A large area plastic scintillation detector with 4-corner-readout *

Shu-Wen Tang(唐述文)[1] Yu-Hong Yu(余玉洪)[1;1)] Yong Zhou(周勇)[1,2] Zhi-Yu Sun(孙志宇)[1]
Xue-Heng Zhang(章学恒)[1] Shi-Tao Wang(王世陶)[1] Ke Yue(岳珂)[1] Long-Xiang Liu(刘龙祥)[1]
Fang Fang(方芳)[1] Duo Yan(闫铎)[1;2] Yu Sun(孙宇)[1,2] Zhao-Min Wang(王兆民)[1,2]

[1] Institute of Modern Physics, Chinese Academy of Sciences, Lanzhou 730000, China
[2] University of Chinese Academy of Sciences, Beijing 100049, China

Abstract: A 760 mm × 760 mm × 30 mm plastic scintillation detector viewed by photomultiplier tubes (PMTs) from four corners has been developed, and the detector has been tested with cosmic rays and γ rays. A position-independent effective time $T_{\rm eff}$ has been found, indicating this detector can be used as a TOF detector. The hit position can also be reconstructed by the time from the four corners. A TOF resolution of 236 ps and a position resolution of 48 mm have been achieved, and the detection efficiency has also been investigated.

Keywords: scintillation detector, 4-corner-readout, time resolution, position resolution

PACS: 29.40.Mc **DOI:** 10.1088/1674-1137/40/5/056001

1 Introduction

With the development of the time-of-flight (TOF) technique, plastic scintillators are widely used in modern nuclear physics laboratories, due to their fast time response, relatively low cost and easy fabrication into a variety of forms useful for many experiments. Recently, numerous large plastic scintillation spectrometers for detection of charged particles and neutrons with energy from tens to hundreds MeV per nucleon have been reported [1–5]. Such detectors are normally placed far (>10 m) downstream from the reaction target. As a result, it is essential to use a large size detector to have a large enough acceptance area. One typical design is to use a modular array. This consists of a number of long plastic scintillator bars viewed by two photomultiplier tubes (PMTs), one at each end. This type of detector always gives good time resolution (typically σ=150 ps) and acceptable position resolution (typically σ=3 cm, along the long direction of the bar). Besides, multi-hit events can easily be handled because of the segmented construction. However, one big problem always exists in this modular design. A large number of bars, equivalently a large number of PMTs and associated electronics channels, means a very high cost and a lot of time-consuming calibration work. One natural way to solve this problem is to use a large volume of plastic scintillator viewed by a minimum number of PMTs.

In this paper, the development of a large area scintillation detector and the results of detailed performance tests with cosmic rays and γ rays are presented.

2 Detector construction

The schematic layout of the detector is shown in Fig. 1. The sensitive area is a 760 mm × 760 mm square and the thickness is 30 mm. The plastic scintillator EJ-200, purchased from the ELJEN Corporation, was chosen as the detection material due to its fast timing (2.1 ns decay time), long optical attenuation length (4 m in bulk) and high scintillation efficiency ($\approx 10^4$ photon / MeV). The square detector was cut off at each corner to form

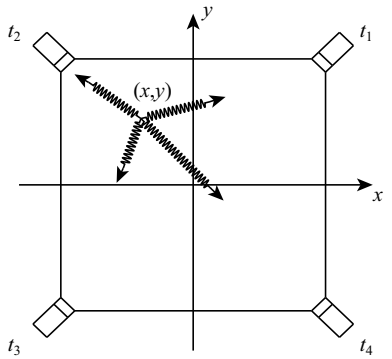

Fig. 1. Schematic layout of the scintillation detector. (x, y) is the hit position of an incident particle, t_1, t_2; t_3, t_4 are the most probable propagation times to reach the four PMTs.

Received 24 August 2015, Revised 1 November 2015
∗ Supported by National Natural Science Foundation of China (U1332207, 11405242)
1) E-mail: yuyuhong@impcas.ac.cn

a plane with a cross section of 42.5 mm × 30 mm. Each plane was glued to a light guide which was mechanically coupled to a Hamamatsu R7724 PMT by means of optical silicone grease. To improve the transmission efficiency of the scintillation light, each surface of the scintillator as well as the light guides was finely polished by the manufacturer. The scintillators and the light guides were first carefully wrapped in a layer of 0.15 mm Tyvek paper, leaving no air gap to give good reflection, and then wrapped with black foam and black tape for light proofing. A high voltage divider circuit was mounted directly behind each PMT. For mechanical protection and light shielding, the readout PMT and its voltage divider were mounted in a PMT housing.

3 Performance of the detector

3.1 Time performance

To investigate the time characteristics of the large area scintillation detector, 49 positions at 7×7 grid points were chosen for study, with every two adjacent grid points separated by an interval of 10 cm. Cosmic ray muons are very suitable for us to study the performance of the square detector as muons lose a fairly constant energy when they pass through the scintillator material. The greatest challenge is that the rate of muons in each measured grid point is too slow, so it would take too long to accumulate enough events. One way to deal with this problem is to test with high rate γ rays for all the 49 points instead, and then do a comparison test with cosmic rays at certain points. Figure 2 shows the schematic layout of the two tests. During the γ ray test (Fig. 2(a)), a lead collimator with a height of 10 cm and hole size of 5 mm in diameter was used for position determination. One of the paired γ rays from a ^{60}Co source went into the upper small trigger scintillator (S1), and the other passed through the collimator hole and was then detected by the large area scintillation detector. During the cosmic ray test (Fig. 2(b)), three small trigger scintillators (S1, S2 and S3) were applied to electronically collimate the muons with triple coincidence. Each of the trigger detectors was constructed from a piece of 2 cm× 2 cm× 1 cm BC-408 plastic scintillator coupled with a Hamamatsu

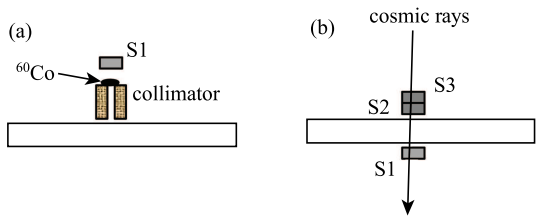

Fig. 2. Schematic layout of the detector tests: (a) test with a ^{60}Co γ source; (b) test with cosmic rays.

R7525 PMT. Different positions of the large area scintillation detector could be tested by moving the trigger detectors. Both of the tests used a CAMAC-CC32 system for data acquisition. The time information from all of the PMT signals was recorded in a Phillips 7186 TDC, and the start timing was made by the trigger detectors.

Rather strong position-dependent time results were observed for all PMTs of the large area scintillation detector. Figure 3 shows that the time information from each PMT varies with the distance to the tested position, which can be described with Eq. 1:

$$t = \delta t + \frac{l}{v_{\rm eff}}, \tag{1}$$

where l is the distance from the tested position to the PMT, $v_{\rm eff}$ is the effective light velocity, and δt is the time delay by the PMT and electronics. The effective light velocities obtained from the PMTs are 15.0 cm/ns, 15.2 cm/ns, 14.9 cm/ns and 15.8 cm/ns, respectively, according to the linear fit results of the experimental data from Fig. 3.

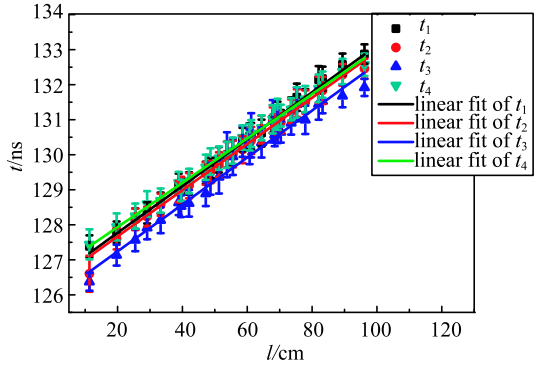

Fig. 3. (color online) Position-dependent time for the PMTs of the detector.

The effective time $T_{\rm eff}$ can be obtained from Eq. 2, following Ref. [6]. Here, the average velocity value $v_{\rm eff}$ = 15.2 cm/ns was applied as a constant for the whole detector.

$$T_{\rm eff} = \frac{1}{4}\sum_{i=1}^{4} T_i - \frac{v_{\rm eff}}{16a}[(T_3 - T_1)^2 + (T_4 - T_2)^2] \tag{2}$$

where a is the half diagonal length of the detector, T_i are the output times from the four corner PMTs, and the subscripts 1, 3 and 2, 4 refer to diagonally opposite corners (see Fig. 1). T_i can be calculated from $T_i = t_i - \delta t_i$, where t_i and δt_i respectively correspond to TDC time and zero time obtained from PMT$_i$. The results of $T_{\rm eff}$ for all tested positions are plotted in Fig. 4. Each of the results is filled in a curly brace and drawn at the corresponding tested grid point. The upper value in the curly

brace is $T_{\rm eff}$ and the lower value is the time resolution (σ), both of them in nanoseconds. The average $T_{\rm eff}$ value is 3.471 ns with RMS of 111 ps, and the average σ value is 375 ps with RMS of 55 ps. Considering the value of time resolution, we can claim that $T_{\rm eff}$ is position-independent over the whole detector range.

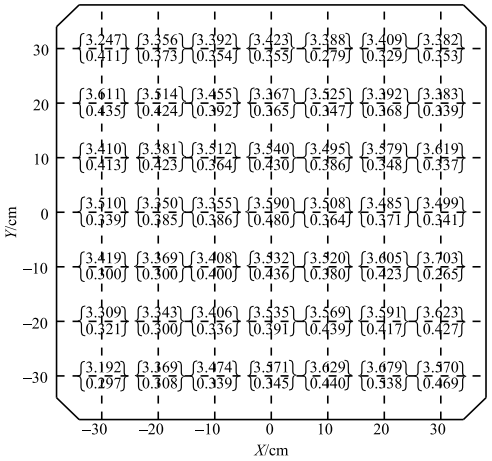

Fig. 4. The effective time $T_{\rm eff}$ and the time resolution (σ) at all grid positions tested with γ rays. All values are in nanoseconds.

Cosmic ray tests were made at three positions of the large detector, one in the center, another at the bottom edge and the last one in the left bottom corner. The comparison results show that the propagation time of the scintillation light from its generated position to each PMT of the detector is equivalent between the cosmic ray test and γ-ray test at every tested position, but the time resolutions from cosmic ray tests are all better because of the certain energy loss in the detector material and the mono generation mechanism of the scintillation light for cosmic rays. Figure 5(a) shows the $T_{\rm eff}$ spectrum for the cosmic ray test and γ-ray test at the center position.

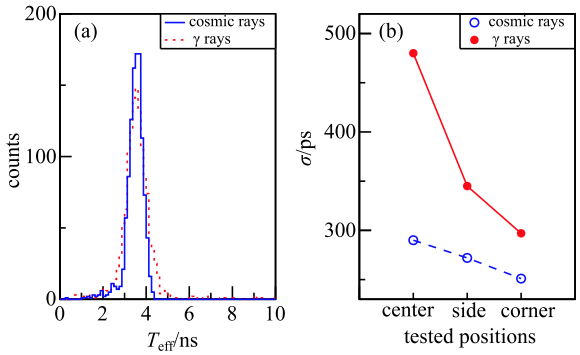

Fig. 5. (color online) (a) $T_{\rm eff}$ distribution for cosmic rays and γ rays tests at the center position of the detector. (b) Time resolution for cosmic ray and γ-ray tests at three tested positions.

The time resolutions from the cosmic ray tests at the three tested points are 290 ps, 272 ps and 251 ps respectively, and the comparison with corresponding γ-ray results is plotted in Fig 5(b). The average time resolution from cosmic rays is 271 ps, which includes the resolution from the trigger detector. After eliminating the contribution of 133 ps from the trigger detector, the average time resolution is 236 ps. According to the time resolution results investigated with γ-rays, the average time resolution of the three positions can almost represent the average time resolution of the whole detector. Therefore, the time resolution for the large scintillation detector is about 236 ps for the cosmic ray test.

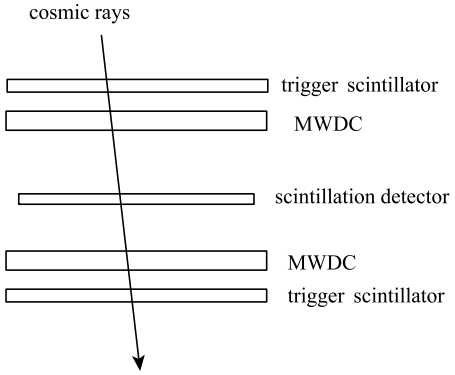

Fig. 6. Schematic layout of position test with cosmic rays.

3.2 Position reconstruction

The detector was tested with cosmic rays in a universal detector test platform, which consists of two multi-wire drift chambers (MWDCs) to determine the trajectory and two large area plastic scintillators as trigger detectors, with the schematic layout shown in Fig. 6. Each of the trigger detectors has an active area of 825 mm× 825 mm, and also has 4-corner-readout by PMTs. The active area of each MWDC is 830 mm× 830 mm and the position resolution is below 1 mm. The detector to be tested was placed in the middle of the platform. If eight PMT signals from both of the upper and lower trigger detectors were all measured at the same time, a valid cosmic ray event was accepted. Then all PMT signals were digitized in a 16-channel high precise HPTDC module [7], and signals from the MWDC wires were recorded in several 128-channel HPTDC modules [8]. As discussed in Section 3.1, the arrival time of each single PMT time is dependent on the hit position. The time difference from the PMTs of the trigger detector can be deduced to be less than 8 ns according to the value of $v_{\rm eff}$ measured before. This causes no trouble for the signals from the MWDCs as the drift time is very slow, but for the fast signal from the scintillation detector, the waggling time of the trigger cannot be negligible so this time is useless

for start timing. However, the HPTDC modules can provide every timing moment with a precision of 24 ps with an internal clock. Therefore, it is unnecessary to use the start timing information. We can use only the four timing moments (T_1, T_2, T_3, T_4) from the corner PMTs to deduce the hit position (x,y).

The time differences from diagonally opposite corners can be expressed with Eq. 3 and Eq. 4:

$$T_3-T_1=\delta t_{31}+\frac{l_3-l_1}{v_{\rm eff}}, \tag{3}$$

$$T_4-T_2=\delta t_{42}+\frac{l_4-l_2}{v_{\rm eff}}, \tag{4}$$

where l_i (i=1, 2, 3, 4) is the distance from the hit position (x,y) to corner i, and δt_{31} and δt_{42} are constants determined by the electronics. If we substitute l_i with corresponding expressions of x and y and solve the equations, the hit position will be obtained. Here we define it as "measured position", labeled as $x_{\rm m}$ and $y_{\rm m}$. The hit position can be also obtained from the two MWDCs through reconstruction of the trajectory of the cosmic ray muons. Because of the high position resolution of the MWDCs, the reconstructed hit position from the two auxiliary detector means the physical location of the incident rays. Here we define such a position as the "true position", labeled as $x_{\rm t}$ and $y_{\rm t}$.

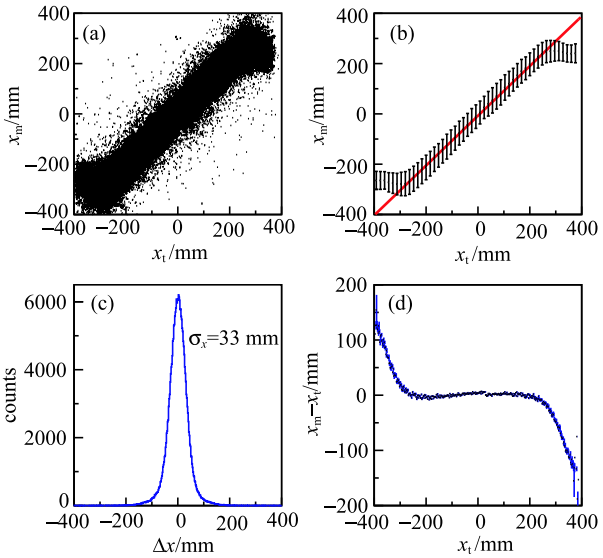

Fig. 7. (color online) Comparison of measured position and real position in the x direction: (a) 2-D scatterplot; (b) position linearity analysis; (c) position resolution; (d) variation with hit position of the deviation between measured and real positions.

Figure 7(a) shows the value of the measured position vs. the value of the true position along the x direction. It shows that the linearity is very good in the central part of the detector but distorted near the edges. With the relation of $x_{\rm m}$ and $x_{\rm t}$, position non-linearity in the x direction can be investigated in the following way. The 2-D spectrum was made from N slices (e.g. $N=50$) along the $x_{\rm t}$ axis, the center of each slice became a new true position x, labeled as $x'_{\rm t}$. Events in each slice were projected to the $x_{\rm m}$ axis to get a new measured position x, labeled as $x'_{\rm m}$. The root mean square (RMS) detector non-linearity (%) for the x direction was determined by Eq. 5:

$$\delta_x=\frac{\sqrt{\langle(x'_{\rm m}-x'_{\rm t})^2\rangle}}{L}, \tag{5}$$

where L is the range in the x direction. Fig. 7(b) shows the position linearity in the x direction; the non-linearity δ_x is 2.8% for the central part of the detector $x_{\rm t}$ from -300 mm to 300 mm, and 7.2% for the whole detector range. As for the y direction, the non-linearity δ_y is 2.9% for $y_{\rm t}$ from −300 mm to 300 mm, and 7.8% for the whole detector range.

The deviation between $x_{\rm m}$ and $x_{\rm t}$ is plotted in Fig. 7(c), which leads to a position resolution of σ_x=33 mm in the x direction, and the position resolution in y direction is similarly obtained as σ_y=35 mm . Therefore, position resolution for the whole detector $\sigma=\sqrt{{\sigma_x}^2+{\sigma_y}^2}$ equals 48 mm.

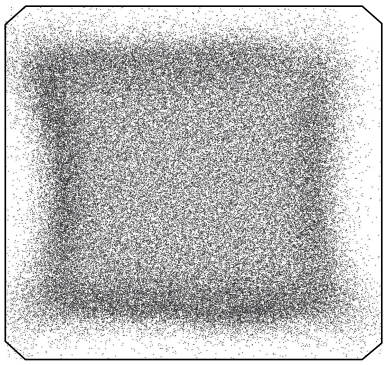

Fig. 8. Position reconstruction from four corner time for cosmic rays.

The variation of deviation with hit position is plotted in Fig. 7(d). The positions reconstructed in the central part of the detector are quite exact, but the deviation becomes larger when cosmic rays hit close to the edges, which is also clearly shown in Fig. 8, a typical position reconstruction for cosmic rays. The positions near every edge of the detector are all mis-reconstructed as being far away from the edge. This is mainly because the photocathodes of the PMTs have limited acceptance angle for the scintillation light. When a cosmic ray hits in one position close to some edge, scintillation light propagated to the neighbouring two PMTs in the shortest path is out of their acceptance angles, and only scintillation light propagated over longer paths can be accepted, which means a

longer time for these PMTs, but scintillation light propagated to the more distant PMTs is not affected. As a result, the position reconstruction presents a tendency to bend the position away from the edge. The regions close to the edges are therefore not suitable for position detection. The effective area of the scintillation detector which can act as a position sensitive detector is about 600 mm× 600 mm in the center.

3.3 Detection efficiency

The detection efficiency at different positions of the detector was also investigated from the cosmic ray test in Fig. 6. The whole detector was divided into enough cells according to the true hit positions of the cosmic ray muons, and in each cell the detection efficiency was calculated as $\eta = N/N_{\rm t}$, where N means the valid number of cosmic ray muons counted with the tested scintillation detector, and $N_{\rm t}$ means the total number of cosmic ray muons counted with the upper and lower trigger detectors. One cosmic ray event was considered valid only when four PMT signals of the tested detector were all detected. Figure 9 shows the detection efficiency of the detector. The detection efficiency is nearly 100% in the main detector range, but decreases dramatically at the edges.

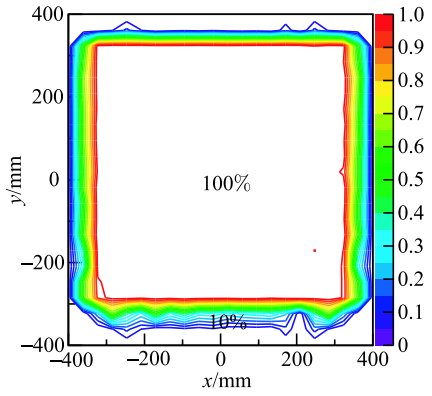

Fig. 9. (color online) Detection efficiency for cosmic rays.

4 Summary and discussion

The construction of a scintillation detector of a size of 760 mm× 760 mm× 30 mm has been described. The time and position performance of the detector have been tested by using γ-rays and cosmic rays. The time information for a single PMT is position-dependent, but a position-independent effective time $T_{\rm eff}$ has been found, which means the detector can be used as a TOF detector, and the TOF resolution is 236 ps as tested with cosmic rays. The position hit by one particle can be reconstructed with the time information from four PMTs in the corners, and the position resolution is 48 mm. The position linearity analysis shows that the non-linearity is about 3% in the center 600 mm region and more than 7% for the whole range. The position reconstruction near the edges has a large deviation mainly caused by the limited acceptance angle of the PMTs. As a position sensitive detector, the effective area of the scintillation detector is about 600 mm× 600 mm in the center. The detection efficiency of the detector is close to 100% in the main detector range, but decreases dramatically at the edges. The counting rate has not been tested due to the limited conditions in the lab, but it is estimated to be less than 10^6 according to Ref. [9], and the actual value will be tested with beams in future.

Compared to a routine TOF detector made of an array of long scintillation bars, the time resolution and position resolution of this detector are slightly worse, and the counting rate is obviously lower because of the holistic volume. The number of readout signals, however, is much less. This detector is much more cost-effective and easier to operate, and could be used in certain nuclear physics experiments which have a not too high counting rate.

We thank the staff of the gas detector lab for their help with the MWDCs.

References

1 M. Baldo-Ceolin, G. Barichello, F. Bobisut et al, Nucl. Instrun. Methods A, **532**: 548 (2004)
2 V. Kouznetsova, A. Lapika, S. Churikova et al, Nucl. Instrun. Methods A, **487**: 396 (2002)
3 P. Grabmayr, T. Hehl, A. Stahl et al, Nucl. Instrun. Methods A, **402**: 85 (1998)
4 Th. Blaich, Th.W. Elze et al, (LAND Collaboration), Nucl. Instrun. Methods A, **314**: 136 (1992)
5 Y.H. Yu, H.G. Xu, H.S. Xu et al, Chin. Phys. C, **33**: 781-784 (2009)
6 J.R.M. Annand, G.I. Crawford, R.O. Owens, Nucl. Instrun. Methods A, **262**: 329 (1987)
7 L. Zhao, L.F. Kang, J.W. Zhou et al, Nucl. Sci. Tech., **25**: 010401 (2014)
8 L.F. Kang, L. Zhao, J.W. Zhou et al, Metrol. Meas. Syst., **20**: 275 (2013)
9 X.H. Zhang, Y.H. Yu, Z.Y. Sun et al, Chin. Phys. C, **37** (5): 056002 (2013)